Wide-Span Multi-Wavelength High-Power Diode-Laser Pumping of Fiber Raman Laser

Soonki Hong, Yutong Feng, and Johan Nilsson

***Abstract*— A multimode silica-core fiber Raman laser was pumped directly by five wavelength-combined multimode diode lasers. The pump wavelengths were spread over a bandwidth of ~700 cm^{-1}, namely, at 976, 969, 950, 940, and 915 nm. This is larger than the Raman peak shift of 490 cm^{-1} . The output power reached 31.5 W with an overall slope efficiency of 42% at the wavelength of 1018 nm when pumped with the maximum launched power of 175 W. According to simulations, the fiber was under-length and the output power could double in a longer fiber. Our results suggest that pumping with spectrally combined diode lasers is a promising approach to high-power fiber Raman lasers, even when the pump wavelengths are not optimized.**

***Index Terms*— Optical fiber lasers, Raman lasers, nonlinear optics.**

I. Introduction

FIBER Raman lasers (FRLs) are acclaimed for their potential as wavelength-agile and efficient brightness enhancers when pumped by multimode pump sources such as diode lasers [1], [2]. The possibility to use well-established silica-based fibers as the gain medium adds to their attraction [3]. However, stimulated Raman scattering (SRS) is a weak nonlinear process compared to ion-based absorption and emission processes and therefore requires much brighter pump sources and longer fibers than what are typically used for rare-earth-doped fiber lasers. Despite these challenges, several recent studies of FRLs pumped by diode lasers have demonstrated power scalability as well as beam quality improvement [1]. Standard telecom graded-index (GRIN) fibers were often selected as the Raman gain fiber (RGF) because of their high quality (notably low loss), low cost, and core parameters compatible with commercial high-power diode lasers for pumping. For example, 154 W was reached in 200 m of germanosilicate GRIN fiber with 65% optical-to-optical efficiency and three times brightness enhancement [4].

These and other similar results were generally obtained with pumping that was spectrally narrow compared to the Raman linewidth of ~80 cm^{-1} for germanosilicate and ~150 cm^{-1} for a pure-silica core. However, our recent experimental work showed efficient Raman conversion is possible with two pumps at wavelengths much further apart. Thus, a germanosilicate GRIN-based FRL reached 23 W of output power with a slope of 50% when pumped simultaneously by two diode lasers at 976 and 950 nm (separation 270 cm^{-1}) [5]. Despite the large separation, the addition of the second diode pump laser more than doubled the output power from that reached with a single diode pump laser. In addition, according to our recent numerical simulations, a total pump bandwidth of ~1000 cm^{-1} still allows for > 60% conversion efficiency [6]. This suggests it is possible to pump fiber Raman lasers with spectrally combined multi-kW diode lasers currently being developed for materials processing with rapidly improving performance and power [7], [8].

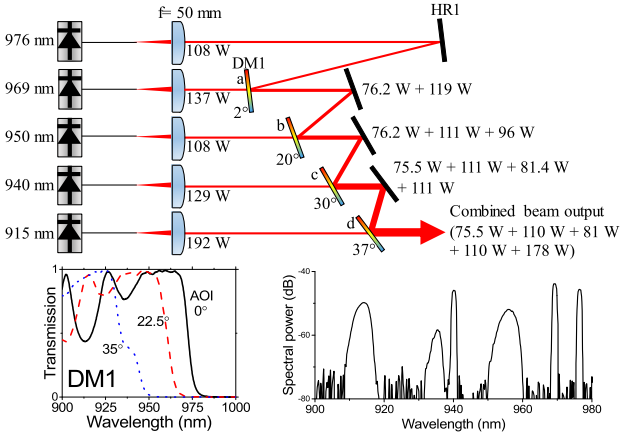

Fig. 1. Layout of spectral combining of pump and the transmission of DM1 as well as the spectrum of the combined beam.

In this letter, we investigate this experimentally, and demonstrate pumping of a FRL with five multimode diode lasers. Each diode laser is spectrally distinct with narrow linewidth, but are spectrally combined into a pump source with total spectral span of 683 cm^{-1}, from 915 nm to 976 nm. This range was limited by the available diode lasers. For the RGF, we used a multimode silica-core step-index fiber. This increases the Raman linewidth, but the absence of Ge reduces the Raman gain compared to telecom GRIN fibers. We did not reach threshold with single wavelength pumping, but with multi-wavelength pumping, with all diode lasers at full power, we reached 31.5 W of output power at 1018 nm with overall slope efficiency of 0.42.

II. Experimental Setup

The spectrally combined pump source comprised five diode lasers with emission wavelength of 976, 969, 950, 940 and 915 nm. See Fig. 1. The lasers at 976, 969, and 940 nm were wavelength-locked and their emission spectra were therefore more stable and narrow, although the 940-nm laser had significant unlocked emission at shorter wavelengths. All five diodes have 105/125 μm, 0.22 NA pigtails and are specified to have over 95% of the power within an NA of 0.15. The beams were collimated individually with f = 50 mm aspheric lenses.

Manuscript received June 26, 2019; revised November 1, 2019; accepted November 9, 2019. Date of publication November 12, 2019; date of current version December 19, 2019. This work was supported by the Air Force Office of Scientific Research under Grant FA9550-15-1-0041. *(Corresponding author: Soonki Hong.)*

The authors are with the Optoelectronics Research Centre, University of Southampton, Southampton SO17 1BJ, U.K. (e-mail: s.hong@soton.ac.uk).

Color versions of one or more of the figures in this letter are available online at http://ieeexplore.ieee.org.

Digital Object Identifier 10.1109/LPT.2019.2953195

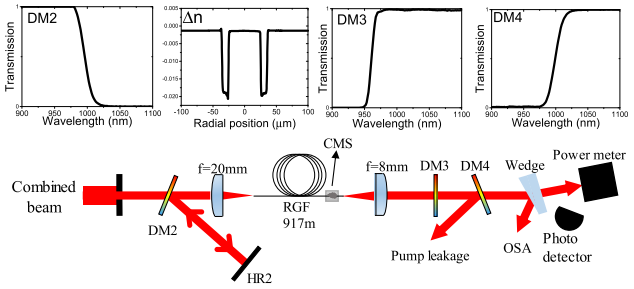

Fig. 2. FRL cavity and measuring positions. Inset graphs depict the transmission of DM2, DM3, and DM4 as well as the index profile of RGF.

This relatively long focal length ensured the pumps remained well collimated over the relatively long free-space beam paths (3 m - 5 m for the different wavelengths). The collimated beams were spectrally combined, one after another from long to short wavelengths, in dichroic mirrors (DM 1). Each mirror transmits the wavelength that is added, and reflects the other wavelengths. The mirrors had the same custom coating but were tuned to different angles-of-incidence (AOIs) from 2° to 37° (specified in Fig. 1) in order to shift the transmission edge. The AOI of each mirror was adjusted in succession to maximize the combined power after the adjusted mirror, with the diode lasers at full power, starting from the longest wavelength. The power reached 555 W (combined), and 76, 110, 81, 110, and 178 W at each wavelength in descending order. This corresponds to an overall combination efficiency of 83%, whereas the combination efficiency of individual diode lasers becomes 70%, 80%, 75%, 85%, and 93%, respectively. The loss of an added wavelength is significant, upon transmission through the DM. The loss of the reflected wavelength closest to the transmission edge is significant, too. The loss of other reflected wavelengths is negligible. It follows that although our angle adjustment approach leads to nearly the maximum combined power, a slightly higher power can be achieved if the transmission edge is shifted towards the shorter, added, wavelength. Since reflected wavelengths suffer no further loss in subsequent mirrors, and since longer-wavelength pump power can be expected to be converted more efficiently to the FRL output, the reflected light is more valuable than that transmitted by a mirror. Thus, the mirror angles should be biased towards low reflection loss. Consequently, there is some limited room for improving the beam combination with the same equipment. In addition, the mirrors can be improved, e.g., with different coatings for different mirrors.

Before the combined pump beam is launched into the RGF it passes through a 10-mm aperture. This clips pump light with poor launch efficiency, which otherwise adds to the thermal load at the launch point. Then, the beam passes through another dichroic mirror (DM2) with 98% transmission for the combined pump beam and $>$ 97% reflection for the Stokes beam at 1018 nm and is launched into the RGF through an f $=$ 20 mm aspheric lens. The incident pump power was measured before the focusing lens to 57, 85, 54, 67, and 96 W in descending wavelength order.

The RGF is 917 m long and is designed for core-pumping. Its 50-μm diameter, 0.227-NA, step-index silica core is surrounded by 10-μm-thick fluorine doped layer and a 345-μm diameter silica cladding. The refractive index profile is shown in Fig. 2. The fiber was pulled in-house from a preform fabricated by Heraeus (Fluosil Q SWS6.95/SWU1.4). The fiber is coated with low-index polymer to reduce the absorption of any light that escapes from the core. Although cladding-guided pump light penetrates into the core and contributes to SRS in the core, the large cladding area makes this effect negligible. Thus, despite the double-clad fiber structure, the pump needs to be launched into the core. The loss of the core was measured to 1.25, 1.28, 1.70, 1.90, 1.50, and 1.07 dB/km at wavelengths of 976, 969, 950, 940, 915, and 1020 nm, by white-light transmission measurements with a cut-back of (nearly) the full length of the fiber. In contrast to GRIN fibers, we do not expect any significant loss difference between core-guided modes. The fiber was perpendicularly cleaved in both ends and a cladding-mode stripper at the far end facilitated core launch alignment and characterization. The pump powers launched into the core were 24.5, 47.5, 21.5, 33.2, and 58.5 W at the different wavelengths in descending order, as calculated from the transmitted power and the fiber background loss. Thus, the launch efficiencies for each wavelength are 43%, 56%, 40%, 50%, and 61%. However there was some crosstalk among the diode lasers, presumably caused by the wavelength drift due to the thermal load so that the total launched power when all the diodes were at their maximum (175 W) was lower than the sum of the powers from each diodes when individually turned on to the maximum (185 W). We compensate for this effect in the data we present. For example, although the launched power from the two longest-wavelength diode lasers in isolation are 24.5 and 47.5 W, with a sum of 72.0 W, the power actually launched became 62.7 W. Thus, the power increment of the second diode laser was not 47.5 W but 38.2 W. This is the power used in presented data, and it is to be understood that the actual launched power at a single wavelength depends on which other wavelengths are present. The adjusted (incremental) launched pump powers were 24.5, 38.2, 20, 37.3, and 54.9 W in descending order of pump wavelengths.

In the far end of the fiber, a collimating lens and a third dichroic mirror (DM3) serves to double-pass the shorter-wavelength pumps at 950, 940, and 915 nm. The reason why we double-pass only the shorter pump wavelengths is that these amplify the longer wavelengths, which can lead to high-power backward-propagating light at long wavelengths. Although it may be possible to avoid this when the laser is operating with substantial amounts of 1st-Stokes power at $\sim$1020 nm, this is challenging to ensure. Thus, initial experiments in which all pump wavelengths were double-passed led to strong backward-propagating 976-nm radiation which damaged the 976-nm diode laser and degraded its power from $\sim$140 W to 108 W. If higher powers are available then the benefits of double-passing the pump become smaller.

To form a cavity for the FRL, a mirror (HR2) back-reflects the beam reflected from DM2 in the pump launch end of the RGF. In this arrangement, the alignment of the launching stage needs to not only optimize the pump launch but also the collimation of the signal beam for efficient feedback of the Raman signal. Therefore, we first maximized the launched pump power, and then realigned the position of the fiber's launch end to maximize the 1st-Stokes SRS, induced by the 976-nm pump and as monitored at the far end output. Then lastly, we optimized the position of each pump pigtail.

In the other end of the cavity, the fiber is perpendicularly cleaved to form a 4%-reflecting output coupler. In addition,

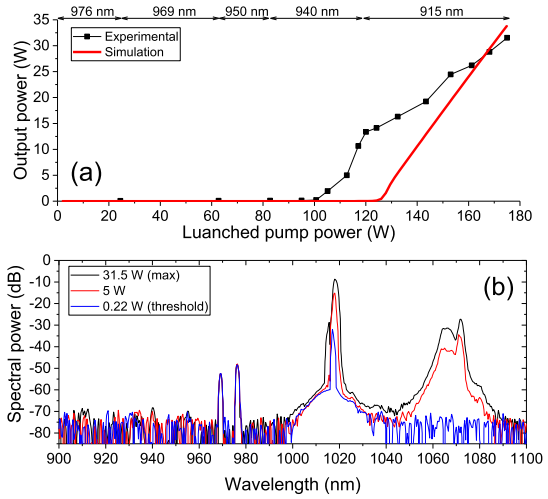

Fig. 3. (a) Output power *vs*. total launched pump power with simulation (b) optical spectra of the output signal measured with 1 nm resolution after DM4, which suppresses the pump waves.

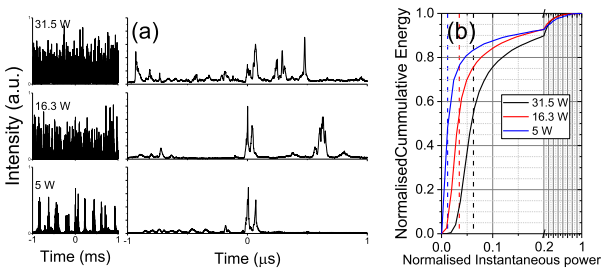

Fig. 4. (a) Temporal traces and (b) normalized cumulative energy *vs*. normalized instantaneous power. Dotted lines depict the average power of each curve.

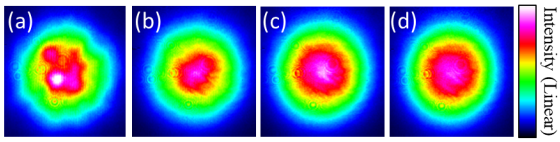

Fig. 5. Beam images of relative intensity at signal output power of (a) 0.3 W, (b) 3.5 W, (c) 16.3 W, and (d) 31.5 W. The intensity is scaled differently in different images.

residual signal reflection from DM3 adds to the feedback, but this was not quantified. A fourth dichroic mirror (DM4) separates leaked pump (976 and 969 nm) from the out-coupled signal. A 4%-reflecting glass wedge samples the out-coupled beam for spectral measurements. The output power was measured with a thermal power meter. A 350-MHz biased silicon photodetector (DET10A, Thorlabs) connected to a 200-MHz oscilloscope (DSO X2022A, Agilent) captured scattered light from the power meter's surface in order to measure temporal traces. We estimate the temporal resolution to 2 ns.

III. Results

We increased the pump power by turning on diodes one by one in descending order of wavelength. We reached the FRL threshold when the 4th diode laser at 940 nm was turned on to 48% of its maximum power for 101 W of total pump power (24.5, 38.2, 20.0, and 17.9 W at 976, 969, 950, and 940 nm, respectively. The threshold in simulations is 126 W.) Then, the signal output power increased with average slope of 0.42 and reached 31.5 W when the 940-nm and 915-nm pumps reached their maximum values. This is shown in Fig. 3(a), together with the result of simulations. In detail, the slope pumped by the 940-nm pump is 0.68. The slope for adding the 915-nm pump power is 0.33. The slope efficiency in the range of 113 – 120 W of launched pump reaches 1.12. We note that the nonlinear pump depletion in a FRL means that the slope efficiency can exceed unity over a limited range of powers. Another possible explanation for slope efficiency > 1, as measured, is drifts in wavelength or alignment, which may have affected the launch into the core at high power. The nonlinear character of a FRL makes this difficult to monitor. The residual pump power in the range 960 – 980 nm was measured to 61 - 64 W for all powers above the laser threshold, in fair agreement with simulations (69 – 80 W).

The signal wavelength was 1018 nm (in the 1st-Stokes wavelength range of 969 and 976 nm) and the linewidth was < 2 nm (Fig. 3(b)). Second-order Stokes emission emerged too, in the 1060 - 1075 nm region in the shape of the typical Raman gain curve of silica fiber. The 2nd-Stokes power was no more than ∼3% of the 1st-Stokes power even at maximum pump power. The 2nd-Stokes power is included in the reported laser output powers. If necessary, higher Stokes orders can be suppressed by improved wavelength selection, e.g., in DM 2. Elimination of broadband feedback from perpendicularly cleaved fiber ends can also improve wavelength selection.

Fig. 4(a) shows temporal traces in 2-ms and 2-μs spans. The output signal was pulsing, seemingly randomly without a clear trend. The pulse duration ranged from ∼6 ns to ∼50 ns (full-width at half-maximum) as observed in the 2-μs spans. The maximum instantaneous power within the 2-ms spans was ∼424 ∼470, and ∼505 W at ∼5, 16.3, and 31.5 W of average output power, respectively. In addition, there is a continuous wave (CW) component in the output power, at least at 31.5 W. To assess the power fluctuations, we calculated the cumulative energy against the instantaneous power (Fig. 4(b)) for those three power levels. The distributions are normalized to their maximum instantaneous powers. Some power may be in higher Stokes-orders, which would reduce the power transfer from the pump and effectively clamp the peak power. The fraction of the energy with instantaneous power below half the average power was 15%, 10%, and 4%, and the fraction with instantaneous power below twice the average was 56%, 73%, and 78%. Thus, the power stability increases at higher output power.

Beam images at four different output powers captured by a silicon CCD camera (Thorlabs BC106N-VIS) with 2 ms exposure time are shown in Fig. 5. Near threshold (Fig. 5(a)), the beam profile is non-circular with significant structure. It was also temporally unstable. This may be because near threshold, only a small subset of the fiber modes is excited through the SRS. At higher pump power, more modes are expected to be excited, and furthermore, the images are averaged over a large number of pulses that are generated in 2 ms, according to Fig. 4. Thus, the beam images became closer to circular, smoother, and temporally stable. The beam quality (M^2) was 6.8 at full power (31.5 W) and 6.1 at 16.3 W (equal in orthogonal directions within ∼3%). It could not be measured at lower powers. The beam diameter was measured at the 13.5% intensity-level by a scanning-slit beam

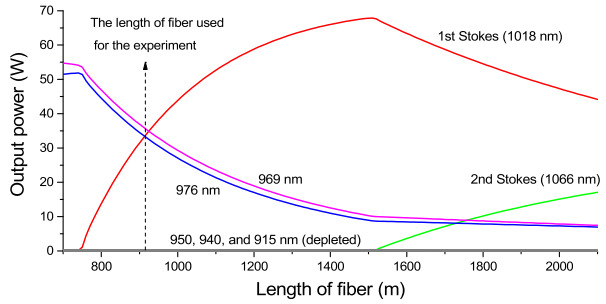

Fig. 6. Simulated output powers in the far end of the fiber (after DM3) *vs.* fiber length. The power at 915, 940, and 950 nm is negligible each wavelength.

TABLE I
PARAMETERS FOR SIMULATION

Parameter	Value	Unit	Parameter	Value	Unit
L_f	917	m	A_{eff}	1964	μm^2
λ_1	1066		r_{f1}	0.9	
λ_2	1018		r_{f2}	0.9	
λ_3	976		r_{f3}	0.04	
λ_4	969	nm	r_{f4}	0.04	
λ_5	950		r_{f5}	0.04	
λ_6	940		r_{f6}	0.04	
λ_7	915		r_{f7}	0.04	
α_1	0.89		r_{b1}	0.04	-
α_2	1.06		r_{b2}	0.04	
α_3	1.21		r_{b3}	0.04	
α_4	1.27	dB/km	r_{b4}	0.04	
α_5	1.72		r_{b5}	0.99	
α_6	1.91		r_{b6}	0.99	
α_7	1.43		r_{b7}	0.99	

Raman gain coefficient ($g_{R_{ij}}$) [fm/W]

	$j=2$	3	4	5	6	7
$i=1$	$g_{R_{ij}}=49.0$	4.52	1.99	1.74	1.63	0.74
2		50.2	45.0	3.91	9.13	2.95
3			9.41	28.7	48.5	4.41
4				18.8	36.4	17.6
5	$(g_{R_{ji}} = g_{R_{ij}})$				12.8	51.2
6						32.3

analyzer on a motorized stage (Thorlabs M2SET-IR). This was controlled by a computer, which also calculated M^2 (Thorlabs Beam Analyzing Software v. 2.3). The M^2-value is markedly lower than the expected $\sim V/2 = 17.5$, if all modes are equally excited.

IV. SIMULATIONS

We used simulations to better understand our system. The model is the same as in ref. [5], except that the effective area was taken to be the same for all wavelengths and the feedback reflectances at both ends were set differently for each wavelength in accordance with the experimental setup.

$$\pm\frac{1}{P_i^{\pm}}\frac{dP_i^{\pm}}{dz} = -\alpha_i + \frac{1}{A_{eff}}\left(\sum_{i>j} g_{R_{ij}}\left(P_j^{+}+P_j^{-}\right) - \sum_{i<j} g_{R_{ij}}\left(\frac{\lambda_j}{\lambda_i}\right)\left(P_j^{+}+P_j^{-}\right)\right),$$
$$with \quad i,j = 1,2,3,4,5,6,7$$

The values of parameters used for the simulation are given in Table I. The parameter r_{fi} and r_{bi} are the launching end and far end reflectances at λ_i. These values were used also for the simulation curve in Fig. 3(a). The simulated output power *vs.* fiber length is shown in Fig. 6. The optimum fiber length is 1510 m, where the 2nd Stokes appears, which we view as undesired. The output power at the optimized length is calculated to 68 W and the pump leakage to 8.8 and 10.1 W for 976 and 969 nm, respectively. All other powers were negligible. This suggests that a longer fiber than we had available, or alternatively a higher pump power, can increase the efficiency.

All simulations are CW and we have not tried to analyze the temporal fluctuations and stability of the system. We note that a coupled nonlinear system may lack stable solutions.

V. CONCLUSION

We demonstrated a fiber Raman laser pumped by spectrally combined multimode diode lasers at five different wavelengths (976, 969, 950, 940, and 915 nm). The laser generated 31.5 W of output power, ~97% of which was in the 1st Stokes order at 1018 nm. The temporal trace showed significant fluctuations, although these became relatively smaller at higher pump power. Simulations suggest the fiber is under-length, and that a longer fiber can increase the output power to 68 W although the pump wavelengths have not been optimized. We believe this is the first demonstration of a fiber Raman laser pumped by a spectrally combined multimode high-power diode laser source with wavelength span greater than the peak Raman shift.

ACKNOWLEDGMENT

The authors would like to thank Dr. Pranabesh Barua for the pulling the Raman gain fiber used in this experiment.

REFERENCES

[1] S. A. Babin, E. A. Zlobina, and S. I. Kablukov, "Multimode fiber Raman lasers directly pumped by laser diodes," *IEEE J. Sel. Topics Quantum Electron.*, vol. 24, no. 3, Jun. 2018, Art. no. 1400310.

[2] T. Yao, A. Harish, J. K. Sahu, and J. Nilsson, "High-power continuous-wave directly-diode-pumped fiber Raman lasers," *Appl. Sci.*, vol. 5, no. 4, pp. 1323–1336, 2015.

[3] V. R. Supradeepa, Y. Feng, and J. W. Nicholson, "Raman fiber lasers," *J. Opt.*, vol. 19, no. 2, 2017, Art. no. 023001.

[4] Y. Glick, V. Fromzel, J. Zhang, N. Ter-Gabrielyan, and M. Dubinskii, "High-efficiency, 154 W CW, diode-pumped Raman fiber laser with brightness enhancement," *Appl. Opt.*, vol. 56, no. 3, pp. B97–B102, 2017.

[5] S. Hong, Y. Feng, and J. Nilsson, "Off-peak dual-wavelength multimode diode-laser- pumped fiber Raman laser," *IEEE Photon. Technol. Lett.*, vol. 30, no. 18, pp. 1625–1628, Sep. 15, 2018.

[6] N. Zhao, S. Hong, A. V. Harish, Y. Feng, and J. Nilsson, "Simulations of multiwavelength cladding pumping of high-power fiber Raman amplifiers," *Opt. Eng.*, vol. 58, no. 10, 2019, Art. no. 102701.

[7] J. Malchus, V. Krause, G. Rehmann, M. Leers, A. Koesters, and D. G. Matthews, "A 40 kW fiber-coupled diode laser for material processing and pumping applications," *Proc. SPIE*, vol. 9348, Mar. 2015, Art. no. 934803.

[8] A. Sanchez-Rubio *et al.*, "Wavelength beam combining for power and brightness scaling of laser systems," *Lincoln Lab. J.*, vol. 20, no. 2, pp. 52–66, 2014.